Dynamic in vitro hemocompatibility of oligoproline self-assembled monolayer surfaces

Mzyk, Aldona; Imbir, Gabriela; Noguchi, Yuri; Sanak, Marek; Major, Roman; Wiecek, Justyna; Kurtyka, Przemyslaw; Plutecka, Hanna; Trembecka-Wojciga, Klaudia; Iwasaki, Yasuhiko

Published in:
Biomaterials Science

DOI:
10.1039/d2bm00885h

Publication date:
2022

Biomaterials Science

ROYAL SOCIETY OF CHEMISTRY

COMMUNICATION

View Article Online
View Journal

Cite this: DOI: 10.1039/d2bm00885h

Received 7th June 2022,
Accepted 19th July 2022

DOI: 10.1039/d2bm00885h

rsc.li/biomaterials-science

Dynamic *in vitro* hemocompatibility of oligoproline self-assembled monolayer surfaces†

Aldona Mzyk,*[a,b] Gabriela Imbir,[a] Yuri Noguchi,[c,d] Marek Sanak,[e] Roman Major,[a] Justyna Wiecek,[a] Przemyslaw Kurtyka,[a] Hanna Plutecka,[e] Klaudia Trembecka-Wójciga,[a] Yasuhiko Iwasaki,[c,d,f] Masato Ueda[c,d] and Sachiro Kakinoki*[c,d,f]

The blood compatibility of self-assembled monolayers (SAMs) of oligoproline, a nonionic antifouling peptide, was investigated using the cone-and-plate assay imitating arterial blood flow conditions. End-capped oligoprolines composed of 6 and 9 proline residues (Pro6 and Pro9) and a Cys residue were synthesized for preparing SAMs (Pro-SAMs) on Au-sputtered glass. The surface of Pro-SAMs indicated hydrophilic property with a smooth topology. The adsorption of blood components and the adhesion of blood cells, including leukocytes and platelets, were strongly suppressed on Pro-SAMs. Moreover, Pro9-SAM did not trigger the activation of platelets (*i.e.*, the conformational change of GPIIb/IIIa and P-selectin (CD62P) expression on platelets and the formation of aggregates). Our results demonstrate that Pro9-SAM completely inhibited acute thrombogenic responses and the activation of platelets under dynamic conditions.

An in-depth characterization of blood-contacting surfaces and a good understanding of dynamic hemocompatibility assays are essential for the successful development and clinical applications of cardiovascular implants.[1–3] The artificial vessels, stents, or elements of heart assist devices with antiadhesive properties that will reduce the risk of coagulation and inhibit soft tissue ingrowth are highly demanded.[4,5] Currently, the most popular antithrombotic implants and devices available on the market are modified by heparin.[6,7] The main disadvantage of heparinization is an increased risk of bleeding.[8] Among the antiadhesive coatings, segmented polyurethane (SPU)-containing polyethylene glycol (PEG) soft segments are used for vascular grafts in clinical practice.[9,10] PEG is gradually removed due to the hydrolysis of SPU, resulting in platelet activation and the induction of immune response.[11,12] The above-mentioned approaches present the main concepts in surface engineering, where the first relies on selective binding of proteins and the second on the nonselective antifouling mode of action.[13–17] As many parameters influence protein adsorption and material interaction with blood, it is very difficult to design bioinert surfaces, which can prevent the adsorption of plasma proteins and thrombosis. Although some platelet activation and aggregate formation pathways are well-described, little is known about how they are modulated by various types of biomaterials.[18,19] The understanding of the mechanism of blood–material interactions at the molecular scale can lead to the utilization of surfaces with a well-defined structure. Self-assembled monolayers (SAMs) on gold are useful to model surfaces since they form such highly ordered systems.[20–22] We previously reported a novel low fouling surface, an oligoproline-based SAMs (Pro-SAMs).[23] Oligoprolines were inspired by the backbone of the amino acid chain of collagen and elastin, proteins of the extracellular matrix. Bioactive short sequences are dispersed within collagen and elastin chains, and the proline-rich backbone does not interfere with their interaction with integrin cell receptors. In our previous work, we demonstrated that Pro-SAMs strongly prevent the adsorption of serum proteins and the adhesion of fibroblasts. Therefore, we hypothesized that Pro-SAMs can be used to obtain a new type of antithrombotic surface. This study resulted in the preparation of Pro-SAMs immobilized with two oligoproline variants of different chain lengths (Ac-Cys-$(Pro)_n$-$CONH_2$ (n = 6 (Pro6) and 9 (Pro9)) on the Au-coated glass surface and an evaluation of their interactions with morphotic blood elements under

[a]*Institute of Metallurgy and Materials Science, Polish Academy of Sciences, Reymonta St. 25, 30-059 Cracow, Poland*
[b]*Department of Biomedical Engineering, University Medical Center Groningen, Antonius Deusinglaan 1, 9713 AW Groningen, Netherlands. E-mail: a.i.mzyk@umcg.nl; Tel: +31 50 361 6094*
[c]*Department of Chemistry and Materials Engineering, Faculty of Chemistry, Materials and Bioengineering, Kansai University, 3-3-35 Yamate-cho, Suita, Osaka 564-8680, Japan. E-mail: sachiro@kansai-u.ac.jp;; Fax: +81 6 6368 3033; Tel: +81 6 6368 3033*
[d]*Organization for Research and Development of Innovative Science and Technology, Kansai University, 3-3-35 Yamate-cho, Suita, Osaka, 564-8680, Japan*
[e]*Department of Medicine, Jagiellonian University Medical College, Skawińska St. 8, 31-066 Cracow, Poland*
[f]*Kansai University Medical Polymer Research Center (KUMP-RC), Kansai University, 3-3-35 Yamate-cho, Suita, Osaka 564-8680, Japan*

† Electronic supplementary information (ESI) available. See DOI: https://doi.org/10.1039/d2bm00885h

in vitro dynamic conditions using the cone-and-plate analyzer (Fig. S1†).[24,25]

The surface topography of Pro-SAMs was evaluated based on atomic force microscopy images (Fig. 1A). The average roughness (R_a) of the Au-coated coverslip was about 3.2 ± 1.0 nm. After the immobilization of Pro6 or Pro9, the R_a value slightly increased to around 6.0 nm. The water contact angle measurements showed that the Au-coated surface (unmodified Au) was the most hydrophobic among the tested materials (Fig. 1B). The water contact angle of the unmodified Au-coated surface was about 72.5° ± 5.0°. The immobilization of Pro6 and Pro9 decreased the water contact angle to around 40°. Pro6-SAM and Pro9-SAM surfaces showed wettability similar to that of PU. The chain length of oligoprolines did not significantly influence the wettability of the surface.

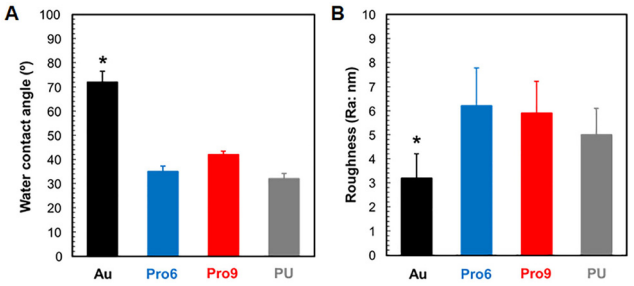

Fig. 1 Surface properties of unmodified Au, Pro6-SAM, Pro9-SAM, and PU surfaces. (A) Water contact angle. (B) Roughness (R_a). The data represent mean ± S.D., n = 6; *p < 0.05 *vs.* PU.

Using the cone-and-plate assay, the surface coverage by morphotic blood elements was determined for the studied materials (Fig. 2A and B). The highest number of adhered blood cells was found on PU. Activated platelets and leukocytes were found at the center of the PU surface more substantially than on the edge of PU. In the case of the Au substrate, the number of morphotic blood elements, which adhered to the central region of the surface, was comparable to what was observed for PU. In comparison to PU, the number of blood cells was lower at the edge. The surface coverage of Pro6-SAM and Pro9-SAM was homogenous. The expression of CD62P (P-selectin), which is a membrane glycoprotein in alpha granules of platelets, was slightly higher on Pro-SAM surfaces than on the Au surface.[26] A similar trend was found for hematopoietic cells, including leukocytes with the expression of CD45.[27–29] The lowest level of vWF, which is secreted by endothelial cells and platelets, was observed on the Pro9-SAM surface (Fig. 2C and D). The surface coverage analysis and the expression levels of the investigated markers showed that the Au surface was covered in the center by a significantly higher number of blood elements compared to oligoproline-based coatings; however, many of them were not activated.

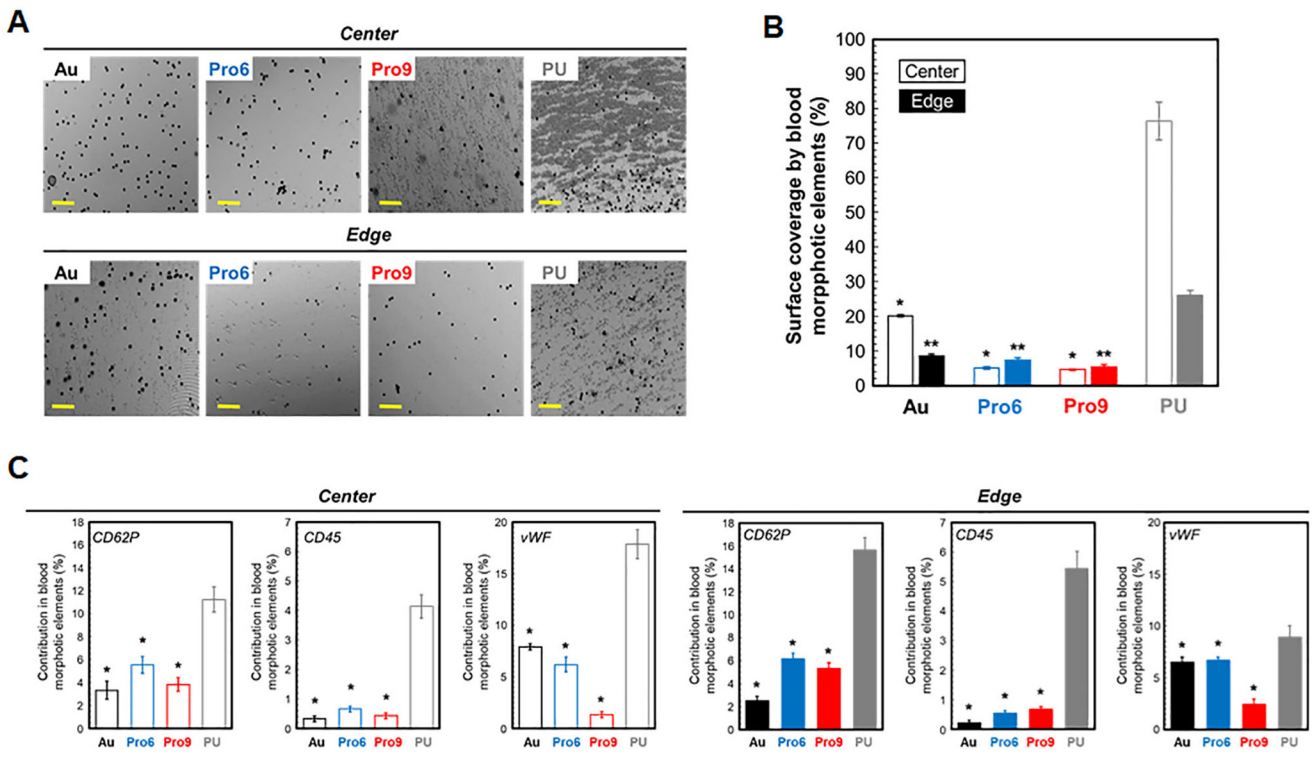

Fig. 2 Coverage of morphotic blood elements on unmodified Au, Pro6-SAM, Pro9-SAM, and PU. (A) Observation of surface coverage at the center and edge of sample surfaces using confocal laser scanning microscopy (scale bar = 100 μm). (B) Surface coverage by morphotic blood elements. The data represent mean ± SD, n = 6; *p < 0.05 *vs.* PU (center), **p < 0.05 *vs.* PU (edge). (C) Contribution of $CD62P^+$ platelets, $CD45^+$ leukocytes, and vWF determined by immunostaining analysis. The data represent mean ± SD, n = 6; *p < 0.05 *vs.* PU.

The changes in blood quality upon contact with the studied surfaces were presented as the expression levels of P-selectin (CD62P) and PAC-1 platelet activation markers, platelet aggregates, as well as the concentration of microparticles (MP), which are fragments of platelets and cell membrane vesicles released during exocytosis in blood plasma (Fig. 3 and 4).[30,31] The number of activated platelets after contact with Pro-SAMs did not increase significantly compared to the level obtained for the baseline control (BASE) (Fig. 3A). The percentage of platelets expressing P-selectin in blood after its activation with ADP was 59.0% ± 1.2% (Fig. 3B). The same marker expression was equal to 0.8% ± 0.3% and 27.9% ± 1.6% for BASE and PU, respectively. The lowest P-selectin level among the selected surfaces was found for Pro9-SAM. The ADP activation changed the number of PAC-1 positive objects in comparison with the donor's blood state. PAC-1 positive platelets were observed at the lowest level in BASE (Fig. 3C). The highest PAC-1 expression was reported for PU (48.0% ± 2.7%). The contact of Pro9-SAM with blood resulted in a lower PAC-1 level compared to the values obtained for PU and Pro6-SAM. The ADP blood treatment did change the MP level in comparison with the donor's blood state, likely due to the rapid aggregation of platelets in the presence of excess ADP. When the shear stress was applied, the MP number slightly increased (Fig. 3D). The concentration of MP also increased on the studied surfaces upon contact with blood. The lowest MP values were found for Pro6-SAM and Pro9-SAM. The trends for aggregate formation were similar to those observed for platelet activation (Fig. 4A–D). The lowest number of platelet–platelet, as well as platelet–monocyte aggregates, was observed for oligoproline-based coatings.

Despite significant advancement in the design of bioinert coatings, a better understanding of the phenomena that occur on the blood–material interface is needed under *in vitro* blood flow conditions. Herein, for the first time, we show that the immobilization of oligoprolines triggers significantly lower platelet adhesion and activation and aggregate formation than the commercially used PU surface, although both surface types demonstrate similar roughness and wettability, indicating that the structure and chemistry of the oligoprolines dictate the antithrombic properties of the oligoproline-immobilized surface.

Our previous study demonstrated that Pro6-SAM and Pro9-SAM form hydrophilic surfaces with a homogenous layer on the Au substrate like the alkane-thiol SAM due to the closely packed oligoprolines having a rod-like structure.[23] Pro6-SAM and Pro9-SAM that were used in this study, indicated a low water contact angle similar to the surface immobilized with ethylene oxide.[32] The surface of Pro-SAMs was very smooth. The average roughness was around 6.0 nm. The topology of

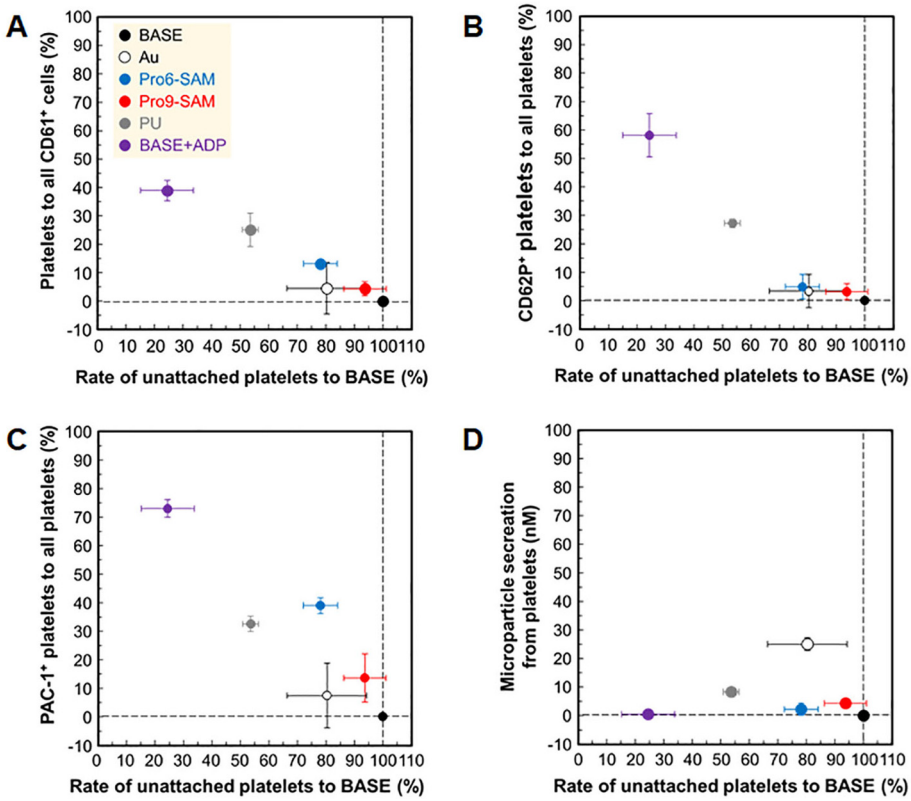

Fig. 3 Surfaces ranked based on the number of (A) CD61 positive platelets; (B) P-selectin positive platelets; (C) PAC-1 positive platelets, and (D) microparticles (MP) in the blood after the cone-and-plate test. All values are plotted against the percentage of remaining platelets after the shear stress (PLT). The data represent mean ± SD, n = 6.

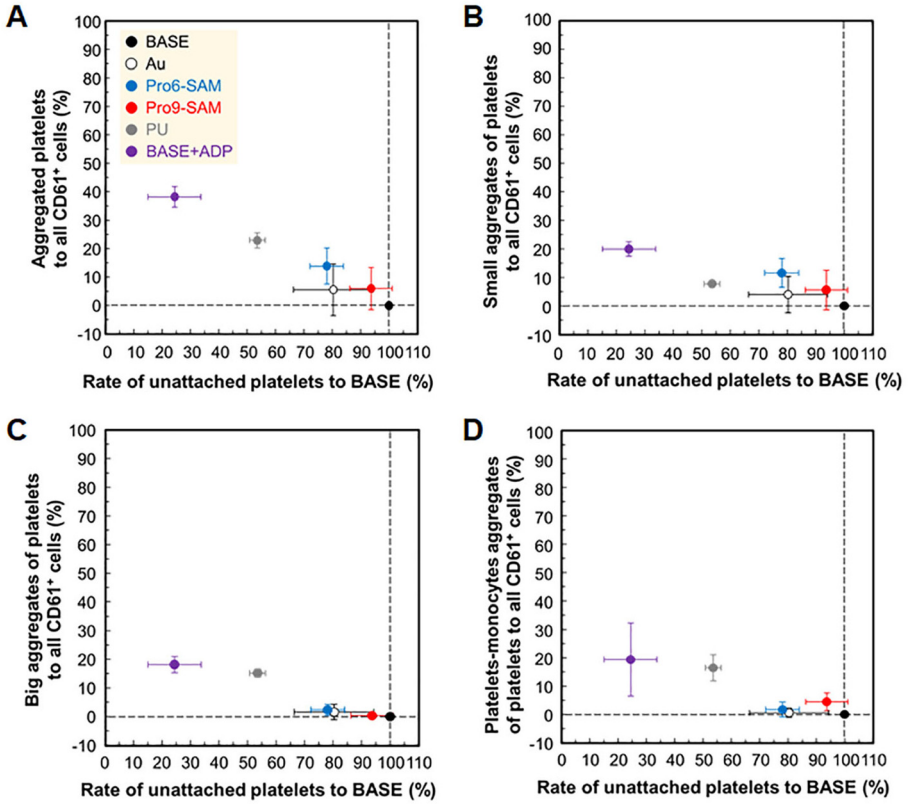

Fig. 4 Surfaces ranked based on the number of (A) platelet aggregates (PLT-AGG), (B) small platelet aggregates, (C) big platelet aggregates, and (D) platelet–monocyte aggregates (PLT-MON-AGG) in the blood after the cone-and-plate test. All values are plotted against the percentage of remaining platelets after the shear stress (PLT). The data represent mean ± SD, n = 6.

Pro-SAMs might not affect their blood compatibility because Scopelliti *et al.* reported that the increased nanoscale roughness from 15 nm to 30 nm induced an increase in the adsorption of fibrinogen and albumin.[33]

Pro-SAMs demonstrated low protein adsorption. The human fibrinogen adsorption on Pro6-SAM and Pro9-SAM was 101.82 and 35.23 ng cm^{-2}, respectively.[23] We did not observe the adsorption of blood components, including fibrin clots, at both the center or edge of Pro6-SAM and Pro9-SAM surfaces upon contact with whole blood under dynamic conditions, as shown in Fig. 2. Tsai *et al.* reported that a low level of fibrinogen adsorption (*ca.* 4.6 ng cm^{-2}) is sufficient for mediating platelet adhesion.[34] However, the orientation of adsorbed fibrinogen on material surfaces influences platelet adhesion and activation more than its amount.[35] Zhang *et al.* reported that the αC region of fibrinogen is preferentially adsorbed on hydrophilic surfaces, thereby exposing the D and E regions containing the platelet biding sequence. In the case of Pro9-SAM, very low platelet adhesion and activation were found even though the amount of fibrinogen adsorption was adequate for mediating platelet adhesion. The results suggested that the orientation of adsorbed fibrinogen on Pro9-SAM may be different than that typically observed on hydrophilic surfaces.

Studies on SAMs functionalized with specific functional groups have shown that, after whole blood incubation, surfaces with methyl groups showed increased platelet adhesion, whereas leukocytes adhered to only hydroxyl-terminated SAMs.[36,37] In contrast, neither platelets nor leukocytes adhered to carboxyl-terminated surfaces.[38] We observed that Pro-SAMs exposing noncharged C-terminal amide groups prevented platelet and leukocyte adhesion. Moreover, the effect of inhibition was related to the length of the peptide chain. Pro9 formed a highly packed SAM layer with higher hydration compared to Pro6 due to the stabilization of the rod-like polyproline-II structure.[39,40] Water molecules, then, might mediate adsorbed blood plasma proteins based on their type and conformation.[41,42] Interestingly, a previous study reported that stable hydration networks are constructed around the polyproline-II structure.[43] The rod-like polyproline-II structure facilitates water molecules to directly access the carbonyl oxygen atoms of Pro residues, which is incorporated into a sheath comprising hydration shells. Hence, the interfacial water molecules might play a crucial role in antifouling properties of Pro-SAMs.

This is the first study to investigate the *in vitro* blood compatibility of Pro-SAMs under dynamic conditions. Surfaces of Pro-SAMs with a smooth topology were prepared by oligoprolines with different chain lengths, the end-capped Ac-Cys-

$(Pro)_6$-$CONH_2$ (Pro6) and Ac-Cys-$(Pro)_9$-$CONH_2$ (Pro9). The adsorption of blood components and platelet adhesion were suppressed on Pro-SAMs compared to the Au substrate and the commercially used PU. Interestingly, the platelets remained nonactivated after contacting with Pro-SAMs, and this tendency was more pronounced for Pro9-SAM than Pro6-SAM. The results demonstrated that excellent blood-compatible surfaces can be fabricated *via* Pro9 immobilization. Further analyses are needed to elucidate the detailed mechanisms of the antifouling characteristics of the Pro9-SAM surface, for example, the interaction with water molecules and small free fatty acids.

Ethical statement

All experiments used human blood were performed in accordance with the Guidelines of International Organization for Standardization (ISO) on testing medical materials that have contact with circulating blood (ISO 10933-4), and approved by the polish center for accreditation (certificate of accreditation of the research laboratory No. AB 120).

Author contributions

Aldona Mzyk: conceptualization, methodology, investigation, supervision, writing: original draft. Gabriela Imbir: investigation, data curation, visualization, writing, review & editing. Yuri Noguchi: investigation. Marek Sanak: investigation, methodology. Roman Major: data curation, formal analysis, investigation, methodology, funding acquisition. Justyna Wiecek: data curation. Przemyslaw Kurtyka: investigation, methodology. Hanna Plutecka: data curation, formal analysis, investigation, methodology. Klaudia Trembecka-Wójciga: data curation. Yasuhiko Iwasaki: methodology. Masato Ueda: methodology. Sachiro Kakinoki: conceptualization, methodology, investigation, visualization, supervision, writing – original draft, funding acquisition. All authors have approved the final version of the manuscript.

Conflicts of interest

There are no conflicts to declare.

Acknowledgements

Statutory funding from IMMS PAS (Z-3) and the project entitled "Nonthrombogenic metal–polymer composites with adaptable micro and macro flexibility for the next generation heart valves in artificial heart devices" (grant number DZP/M-ERA.NET-2014/291/2015) funded by the Polish National Centre of Research and Development are acknowledged. A part of this research was supported by JSPS KAKENHI (grant number JP18K05196 and JP22H03929).

References

1 C. L. Haycox and B. D. Ratner, *J. Biomed. Mater. Res.*, 1993, **27**, 1181–1193.
2 M. Nalezinková, *Thromb. Res.*, 2020, **195**, 146–150.
3 W. H. De Jong, J. W. Carraway and R. E. Geertsma, In Vivo and in Vitro Testing for the Biological Safety Evaluation of Biomaterials and Medical Devices, in *Biocompatibility and Performance of Medical Devices*, ed. J. P. Boutrand, Elsevier Ltd., Amsterdam, 2020, pp. 123–166.
4 D. F. Howe, C. W. Svare and R. W. Tock, *J. Biomed. Mater. Res.*, 1974, **8**, 399–406.
5 T. D. Estridge and D. S. Feldman, *J. Biomater. Appl.*, 1991, **6**, 157–169.
6 R. A. Hoshi, R. Van Lith, M. C. Jen, J. B. Allen, K. A. Lapidos and G. Ameer, *Biomaterials*, 2013, **34**, 30–41.
7 R. Biran and D. Pond, *Adv. Drug Delivery Rev.*, 2017, **112**, 12–23.
8 A. Krishnaswamy, A. M. Lincoff and C. P. Cannon, *Crit. Pathw. Cardiol.*, 2010, **9**, 35–40.
9 J. Chlupác, E. Filová and L. Bačáková, *Physiol. Res.*, 2009, **58**, 119–140.
10 J. D. Kakisis, C. D. Liapis, C. Breuer and B. E. Sumpio, *J. Vasc. Surg.*, 2005, **41**, 349–354.
11 P. Zhang, F. Sun, S. Liu and S. Jiang, *J. Controlled Release*, 2016, **244**, 184–193.
12 G. T. Kozma, T. Shimizu, T. Ishida and J. Szebeni, *Adv. Drug Delivery Rev.*, 2020, 163–175.
13 S. C. Freitas, S. Maia, A. C. Figueiredo, P. Gomes, P. J. B. Pereira, M. A. Barbosa and M. C. L. Martins, *Acta Biomater.*, 2014, **10**, 1227–1237.
14 S. C. Freitas, T. B. Cereija, A. C. Figueiredo, H. Osório, P. J. B. Pereira, M. A. Barbosa and M. C. L. Martins, *Acta Biomater.*, 2012, **8**, 4101–4110.
15 K. Ishihara, S. Tanaka, N. Furukawa, K. Kurita and N. Nakabayashi, *J. Biomed. Mater. Res.*, 1996, **32**, 391–399.
16 K. Ishihara, *Langmuir*, 2019, **35**, 1778–1787.
17 C. Werner, M. F. Maitz and C. Sperling, *J. Mater. Chem.*, 2007, **17**, 3376–3384.
18 M. Jin, W. Chen, W. Huang, L. Rong and Z. Gao, *Acta Pharm. Sin. B.*, 2013, **3**, 123–129.
19 S. T. Proulx, P. Luciani, A. Christiansen, S. Karaman, K. S. Blum, M. Rinderknecht, J. C. Leroux and M. Detmar, *Biomaterials*, 2013, **34**, 5128–5137.
20 S. Margel, E. A. Vogler, L. Firment, T. Watt, S. Haynie and D. Y. Sogah, *J. Biomed. Mater. Res.*, 1993, **27**, 1463–1476.
21 T. Riedel, Z. Riedelová-Reicheltová, P. Májek, C. Rodriguez-Emmenegger, M. Houska, J. E. Dyr and E. Brynda, *Langmuir*, 2013, **29**, 3388–3397.
22 S. Kakinoki, N. Yui and T. Yamaoka, *J. Biomater. Appl.*, 2013, **28**, 544–551.
23 Y. Noguchi, Y. Iwasaki, M. Ueda and S. Kakinoki, *J. Mater. Chem. B*, 2020, **8**, 2233–2237.
24 A. Mzyk, G. Imbir, K. Trembecka-Wójciga, J. M. Lackner, H. Plutecka, E. Jasek-Gajda, J. Kawałko and R. Major, *ACS Biomater. Sci. Eng.*, 2020, **6**, 898–911.

25 R. Major, M. Kopernik, A. Kuźmińska, G. Imbir, H. Plutecka, M. Pomorska, T. Ciach and J. M. Lackner, *Colloids Surf., B*, 2021, **199**, 111562.
26 J. Curvers, J. De Wildt-Eggen, J. Heeremans, J. Scharenberg, D. De Korte and P. F. Van Der Meer, *Transfusion*, 2008, **48**, 1439–1446.
27 A. Nakano, T. Harada, S. Morikawa and Y. Kato, *Pathol. Int.*, 1990, **40**, 107–115.
28 U. M. Vischer and J. Thromb, *Haemostasis*, 2006, **4**, 1186–1193.
29 C. Kawecki, P. J. Lenting and C. V. Denis, *J. Thromb. Haemostasis*, 2017, **15**, 1285–1294.
30 S. J. Shattil, M. Cunningham and J. A. Hoxie, *Blood*, 1987, **70**, 307–315.
31 S. Nomura, T. Nakamura, J. Cone, N. N. Tandon and J. Kanibayashi, *Cytometry*, 2000, **40**, 173–181.
32 C. Pale-Grosdemange, E. S. Simon, K. L. Prime and G. M. Whitesides, *J. Am. Chem. Soc.*, 1991, **113**, 12–20.
33 P. E. Scopelliti, A. Borgonovo, M. Indrieri, L. Giorgetti, G. Bongiorno, R. Carbone, A. Podestà and P. Milani, *PLoS One*, 2010, **5**, e11862.
34 W. B. Tsai, J. M. Grunkemeier, C. D. McFarland and T. A. Horbett, *J. Biomed. Mater. Res.*, 2002, **60**, 348–359.
35 L. Zhang, B. Casey, D. K. Galanakis, C. Marmorat, S. Skoog, K. Vorvolakos, M. Simon and M. H. Rafailovich, *Acta Biomater.*, 2017, **54**, 164–174.
36 V. A. Tegoulia and S. L. Cooper, *J. Biomed. Mater. Res.*, 2000, **50**, 291–301.
37 J. N. Barbosa, M. C. L. Martins, S. C. Freitas, I. C. Gonçalves, A. P. Águas and M. A. Barbosa, *J. Biomed. Mater. Res., Part A*, 2010, **93**, 12–19.
38 C. Sperling, R. B. Schweiss, U. Streller and C. Werner, *Biomaterials*, 2005, **26**, 6547–6557.
39 S. Kakinoki, Y. Hirano and M. Oka, *Polym. Bull.*, 2005, **53**, 109–115.
40 S. Kakinoki, M. Kitamura, Y. Noguchi and Y. Arichi, *Pept. Sci.*, 2020, **112**, e24170.
41 H. Kitano, S. Tada, T. Mori, K. Takaha, M. Gemmei-Ide, M. Tanaka, M. Fukuda and Y. Yokoyama, *Langmuir*, 2005, **21**, 11932–11940.
42 J. Jin, W. Jiang, J. Yin, X. Ji and P. Stagnaro, *Langmuir*, 2013, **29**, 6624–6633.
43 K. Okuyama, C. Hongo, G. Wu, K. Mizuno, K. Noguchi, S. Ebisuzaki, Y. Tanaka, N. Nishino and H. P. Bächinger, *Biopolymers*, 2009, **91**, 361–372.

